

2008

Raman study of element doping effects on the superconductivity of MgB₂

Wenxian Li

University of Wollongong, wenxian@uow.edu.au

Yongqing Li

Shanghai University

R H. Chen

University of Wollongong

Rong Zeng

University of Wollongong, rzeng@uow.edu.au

S. X. Dou

University of Wollongong, shi@uow.edu.au

See next page for additional authors

Follow this and additional works at: <https://ro.uow.edu.au/engpapers>



Part of the [Engineering Commons](#)

<https://ro.uow.edu.au/engpapers/3353>

Recommended Citation

Li, Wenxian; Li, Yongqing; Chen, R H.; Zeng, Rong; Dou, S. X.; Zhu, M Y.; and Jin, H M.: Raman study of element doping effects on the superconductivity of MgB₂ 2008, 094517-1-094517-7.
<https://ro.uow.edu.au/engpapers/3353>

Authors

Wenxian Li, Yongqing Li, R H. Chen, Rong Zeng, S. X. Dou, M Y. Zhu, and H M. Jin

Raman study of element doping effects on the superconductivity of MgB_2

W. X. Li,^{1,2} Y. Li,² R. H. Chen,^{1,2} R. Zeng,¹ S. X. Dou,^{1,*} M. Y. Zhu,² and H. M. Jin²

¹*Institute for Superconducting and Electronic Materials, University of Wollongong, Wollongong, NSW 2522, Australia*

²*School of Materials Science and Engineering, Shanghai University, 149 Yanchang Road, Shanghai 200072, People's Republic of China*

(Received 3 October 2007; revised manuscript received 20 December 2007; published 25 March 2008)

The influences of phonon frequency and unit cell volume on the superconductivity of element-doped MgB_2 are discussed with reference to a Raman study on SiC, C, Mn, and Al-Ag-doped Mg-B materials. A phenomenon has been found in the doped samples, in that the phonon frequency changes to counteract the crystal lattice variation to keep the system stable within a Grüneisen parameter of 2.0–4.0. The chemical doping effects on phonon frequency and unit cell volume can be explained by the harmonicity-anharmonicity competition in the compounds. A decreased electronic density of states is responsible for the depression of superconductivity that is seen in doped MgB_2 . The possibility of a high critical temperature, T_c , in the Mg-B system exists if the material can possess both a high phonon frequency and a big unit cell volume at the same time, as indicated by the isotope effect and hydrogenation experiments.

DOI: [10.1103/PhysRevB.77.094517](https://doi.org/10.1103/PhysRevB.77.094517)

PACS number(s): 74.70.Ad, 74.62.Dh, 74.25.Jb, 78.30.Er

The discovery of superconductivity at 40 K in MgB_2 (Ref. 1) has attracted intense scientific interest towards modifying the structural and electronic properties of this material to improve its critical transition temperature T_c . Although some possible routes to increase the T_c ,^{2–7} such as increasing the phonon frequency, increasing the density of states, and expanding the unit cell volume, have been employed in the Mg-B system, all attempts to modify the MgB_2 host lattice to further increase T_c have failed. It seems that most factors which influence the superconductivity of MgB_2 have already been optimized in the pure Mg-B system. Chemical substitution, a method to change several physical properties, such as the electron density, crystal lattice parameters, and the disorder effect, has been well investigated by different groups. On the fact of T_c depression, Takenobu *et al.*⁸ and Lee *et al.*⁹ explain it as due to crystal lattice contraction, electron doping induced electronic structure variation, and the disorder effect arising from substitution, while Kortus *et al.*¹⁰ ascribe the T_c depression to band filling and interband scattering effects. It should be noted that Kazakov *et al.*⁷ have suggested that the main issue is the competition between the effects of atomic size disorder, which causes the T_c to decrease, and those of crystal lattice expansion, which tends to increase T_c , which is in agreement with the positive T_c dependence on unit cell volume for MgB_2 samples under pressure, as estimated by Deemyad *et al.*¹¹ However, in the case of Ag and Al codoped MgB_2 [$\text{Mg}_{1-2x}(\text{AgAl})_x\text{B}_2$], the a -axis and c -axis parameters increase with doping, and the volume V also increases, while the T_c decreases with doping.³ The authors attribute these characteristics to a disorder effect caused by the chemical substitution.³ In a phonon-mediated superconductor,¹² it is well known that the T_c is proportional to the averaged phonon frequency $\langle\omega\rangle$, according to the McMillan formula. Factor group analysis predicts four modes at the Γ point of the Brillouin zone for the $P6/mmm$ space group in MgB_2 : a silent B_{1g} mode, the E_{2g} Raman mode, and the infrared active E_{1u} and A_{2u} modes. Only the E_{2g} mode is Raman active and strongly coupled to the electronic conduction σ bands. The high T_c for MgB_2 is partially attributed to the strong intensity of electron-phonon

coupling due to the high frequency of the E_{2g} phonon mode.^{10,13}

Chemical substitution is expected to modify the phonon spectrum, by diversifying the phonon frequency and electron-phonon coupling strength.¹⁴ Carbon substitution effects on the superconductivity have been studied widely,^{15–18} because carbon is believed to be one of the most effective elements for incorporation into the MgB_2 lattice.¹⁹ The E_{2g} phonon peak shifts to the higher energy side, and the peak is narrowed with increasing x in $\text{Mg}(\text{B}_{1-x}\text{C}_x)_2$.^{15–18,20} The increased E_{2g} peak energy and narrowing of the peak width suggests the weakening of electron-phonon coupling by C substitution.¹⁷ The effects of C substitution are an increase in impurity scattering and band filling, which reduces the density of states and alters the shape of the Fermi surface. The decrease in T_c in C-doped samples is mainly attributed to the decreased density of states and changes in phonon modes,¹⁰ while the increased scattering also contributes to the T_c reduction, mainly at low doping concentrations. As a carbon source, nano-SiC has proved to be one of the most effective substitution dopants for improving the critical current density (J_c), irreversibility field (H_{irr}), and upper critical field (H_{c2}) in MgB_2 since the discovery of superconductivity in this material.²¹ In spite of intensive studies on the transport properties of SiC-doped MgB_2 , the mechanism explaining why SiC doping is special remains unclear, especially since there has not been adequate research on its effects on the superconductivity. In this work, the T_c dependence on the phonon frequency and unit cell volume is researched systematically to explain the mechanism responsible for the superconductivity depression with different SiC doping levels in MgB_2 . Furthermore, to find out how variation of the unit cell volume and the frequency of the E_{2g} mode affect the superconductivity in doped MgB_2 and to further explore the mechanism of superconductivity, the influence of the phonon frequency and lattice parameters on T_c for SiC-doped MgB_2 are compared with previous work on carbon,^{15,16} Mn,²² and Al-Ag-doped MgB_2 .³ Then the possible origin of high T_c in this material is proposed, based on the isotopic effects and hydrogenation experiments.

MgB_2 superconductor bulks were prepared by an *in situ*

reaction process, using mixed powders of micron size magnesium (99%) and nanosized amorphous boron (99.99%), with different levels of 0, 5, 10, and 15 wt % nanosized SiC (99%). The mixtures were ground sufficiently, using an agate mortar in an argon gas filled glove box, and pressed into bulks with dimensions of 10 mm diameter and about 5 mm thickness under a pressure of ~ 600 MPa. Then the samples were sintered in a tube furnace at 750°C for 30 min, at a heating rate of $5^\circ\text{C}/\text{min}$, and furnace-cooled to room temperature. High purity argon gas flow was maintained throughout the sintering process. A pure MgB_2 sample was synthesized using 10 hours of sintering at 800°C in high purity argon atmosphere. Part of the sample was hydrogenated in 30 atm H_2 atmosphere at 500°C for 2 h to compare the superconductivity, phonon frequency, and unit cell volume.

All samples were characterized by x-ray diffraction (XRD: $D\text{max-2200}$), and the lattice parameters were refined with the aid of JADE 5.0 software. The Raman scattering was measured using a confocal laser Raman spectrometer (Renishaw inVia plus) with a $100\times$ microscope. The 514.5 nm line of an Ar^+ laser was used for excitation, with the laser power maintained at about 20 mW, measured on the laser spot on the samples, in order to avoid laser heating effects on the studied materials. Several spots were selected on the same sample to collect the Raman signals, in order to make sure that the results were consistent. The magnetoresistivity, $\rho(H, T)$, was measured, with H applied perpendicular to the current direction, using the four probe method in the temperature range from 4.2 K to 300 K and a field range from 0 T to 9 T [in a physical properties measurement system (PPMS: Quantum Design)]. The T_c values were deduced from the $\rho(H, T)$ curves. The T_c values of the sample before and after hydrogenation were determined by ac susceptibility measurements executed on the PPMS.

The Raman spectra of pure MgB_2 and SiC-doped MgB_2 , measured at ambient temperature with an excitation wavelength of 514.5 nm, are shown in Fig. 1. Two broadbands centered at about 600 and 800 cm^{-1} are observed for all materials. In pure MgB_2 , the most prominent phonon peak located at lower frequency (centered at $\sim 566\text{ cm}^{-1}$) is assigned to the E_{2g} mode.^{23–26} The high frequency Raman band [centered at 759 cm^{-1} and marked as phonon density of states (PDOS) in Fig. 1] has also been observed earlier in MgB_2 ^{24,27} and attributed to phonon density of states PDOS due to disorder.^{23,28–30} This second peak is responsible for the asymmetric profiles generally reported in the E_{2g} mode frequency region in MgB_2 . The Raman spectra of MgB_2 preserve their main characteristics as the SiC concentration increases, except that there is a new low frequency peak centered at 250 cm^{-1} . This peak arises from the Raman active F_{2g} mode in the cubic structure of Mg_2Si , which is described by the $Fm\bar{3}m$ space group, and its intensity is enhanced with the increasing Mg_2Si content in the compounds. However, the E_{2g} peak of the SiC-doped samples shifts to higher frequency, and its relative intensity and full width at half maximum (FWHM) decrease considerably, as shown in Figs. 1 and 2. At the same time, the peak centered at about 780 cm^{-1} gradually becomes the most prominent feature in the Raman

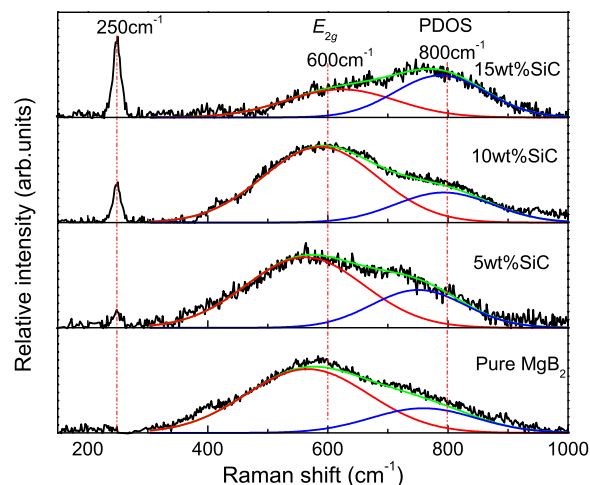


FIG. 1. (Color online) Normalized Raman spectra with Gaussian fitted E_{2g} mode and phonon density of states (PDOS) for 0, 5, 10, and 15 wt % SiC-doped MgB_2 sintered at 750°C for 30 min. The baselines have been subtracted from the patterns.

spectrum at higher doping levels. The FWHM of the E_{2g} peak in pure MgB_2 exceeds 200 cm^{-1} , which is attributed to the presence of strong electron-phonon coupling and phonon-phonon interaction (anharmonicity).^{23,24,28,31,32} The latest calculations demonstrate that the Raman data can be explained if dynamical effects beyond the adiabatic Born-Oppenheimer approximation and electron lifetime effects are included in the phonon self-energy, without invoking anharmonicity.³³ This result is consistent with the harmonic phonon dispersion results measured by inelastic x-ray scattering.^{34–37} As for the 5 wt % SiC-doped sample, its Raman spectrum shows little difference from that of the pure

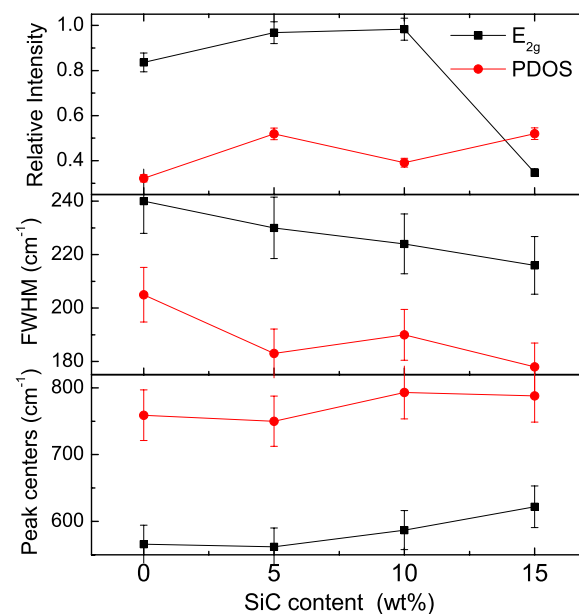


FIG. 2. (Color online) Contrast of relative intensity, FWHM, and peak centers of the E_{2g} mode and PDOS for 0, 5, 10, and 15 wt % SiC-doped MgB_2 sintered at 750°C for 30 min.

MgB₂ because of the low level of both the Mg₂Si inclusions and C substitution for the boron. In the range up to 15 wt % in SiC-doped samples, the E_{2g} peak shifts from 566 cm⁻¹ in pure MgB₂ to 622 cm⁻¹, while the PDOS peak gradually shifts from 759 cm⁻¹ to 788 cm⁻¹, as shown in Fig. 2. This behavior indicates that the band structure of MgB₂ shows a high phonon vibration frequency with the increasing SiC doping levels. This transformation has also been found in C-doped MgB₂ systems and is explained by the C substitution for B in the MgB₂, which causes a lattice relaxation around the C impurity atom because the C-B bond length, about 1.71 Å, is smaller than the B-B bond length (~1.78 Å).¹⁶ However, the SiC-doped MgB₂ shows a sharper rate of increase than in the C-doped samples. This is because the C atoms in SiC are easier to incorporate into the MgB₂ lattice than those from carbon black or graphite. According to the dual reaction model,³⁸ SiC reacts with Mg to release highly reactive C at a low temperature, which is exactly the formation temperature of MgB₂. As a result, the C incorporation into the lattice and the inclusion of nanoparticles of Mg₂Si impurity in MgB₂ grains take place simultaneously. The actual carbon substitution level reached 3.2 at % at the 15 wt % doping level, whereas the actual C substitution from a comparable doping level of nanosize carbon is less than 2 at %, which is also reflected in the smaller variation of the *a*-axis lattice parameter.⁸ Similar behavior was observed earlier in Mg_{1-x}Al_xB₂ superconductors in the high aluminum content region, because of the Al substitution induced lattice shrinkage.²⁷

Although it seems that SiC-, C-, or Al-doped MgB₂ should actually show higher T_c than the pure sample, due to the strong electron-phonon coupling induced by the high phonon frequency, T_c depression occurs in all the small size atom doped systems. In contrast to SiC-, C-, and Al-doped MgB₂, with Al-Ag codoping, the E_{2g} mode shifts to low frequency as the Al-Ag content increases, as observed from Raman spectroscopy.³ The E_{2g} frequency in Al-Ag codoped MgB₂ decreases from 560 cm⁻¹ in pure MgB₂ to about 540 cm⁻¹ in Mg_{0.09}(Al,Ag)_{0.01}B₂. The T_c of element doped MgB₂ deteriorates as the doping level is increased, regardless of the hardening or softening of the frequency of the E_{2g} mode, and is lower than that of the pure MgB₂, 39.4 K, as shown in Fig. 3(a).¹

The analysis of lattice parameters shows a great constriction of the unit cells after SiC substitution, as shown in Table I, which is in accordance with previously reported carbide doped systems.^{9,15,16} This contraction due to chemical substitution corresponds to an application of hydrostatic pressure of 3.5–4.0 GPa.³⁹ Due to the negative pressure coefficient,^{40–45} $dT_c/dP = -1.03 - 2.0$ K GPa⁻¹, the lattice shrinkage degraded the T_c in a similar way to applying ambient pressure on the MgB₂. The frequency of the E_{2g} mode under high pressure shows the same trend as for small size atom element doped MgB₂.⁴⁰ To overcome the influence of the negative pressure coefficient on the superconductivity, the unit cell volume can be expanded via the substitution of atoms with a larger ionic radius, which would be expected to increase the T_c . Although Mn doping can increase the crystal cell volume, T_c decreases sharply with a much more sensitive response than in the cases of C- and Al-doped samples.²²

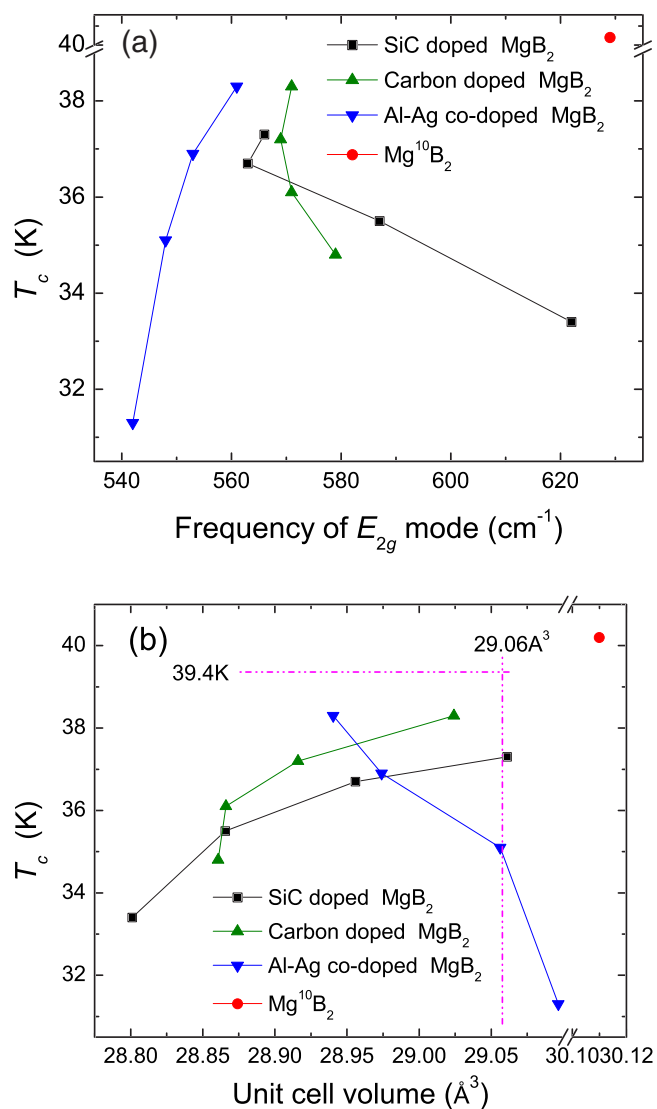


FIG. 3. (Color online) T_c dependence on (a) the frequency of the E_{2g} mode, and (b) the unit cell volume for SiC-, carbon-, and Al-Ag-doped MgB₂, and for Mg¹⁰B₂. The SiC-doped samples were sintered at 750 °C for 30 min. The carbon-doped samples were sintered at 900 °C for 2 h.^{8,15} The Al-Ag-doped MgB₂ was sintered at 950 °C for 1 h.³ The Mg¹⁰B₂ sample was sintered at 950 °C for 2 h,^{40,51} while the magenta lines show the T_c and unit cell volume value of pure MgB₂ in Ref. 1.

The E_{2g} peak remains almost unchanged as the Mn content is experimentally increased to 1 wt %. The authors believe that the Mn substitution does not weaken the electron-phonon coupling for the stable phonon frequency, but rather, electron pairs were destroyed by the magnetism of the Mn atoms. To keep the electronic structure and carrier concentration stable, while expanding the crystal unit cell volume, Al and Ag codoping effects with the same stoichiometric ratio have been explored.³ The crystal lattice expands along both the *a*- and *c*-axis directions, because the average ionic size, 0.843 Å for both Al and Ag, is larger than the ionic size of Mg (0.720 Å), but the T_c is depressed as the doping levels increase. According to the T_c dependence on the unit cell volume, both the volume contraction in SiC- and C-doped

TABLE I. The lattice parameters, actual carbon substitution contents, MgO relative intensity in XRD, and critical temperature (T_c) for undoped and nano-SiC-doped MgB_2 bulks sintered at 750 °C.

Doping level SiC (wt %)	Annealing (°C × min)	Lattice parameters		Unit cell volume (Å ³)	x value in $\text{MgB}_{2-x}\text{C}_x$ ^a	$\frac{I_{\text{MgO}}^{220}}{I_{\text{MgB}_2}^{101}}$ (%) ^b	T_c (K)
		a (Å)	c (Å)				
0	750 × 30	3.08496	3.52610	29.06	—	5.6	37.3
5	750 × 30	3.08134	3.52159	28.96	0.010	4.9	36.7
10	750 × 30	3.07634	3.52204	28.87	0.022	4.8	35.5
15	750 × 30	3.07305	3.52169	28.80	0.032	—	33.4

^aActual carbon substitution content calculation based on the relationship in Ref. 9.

^bThe ratio was calculated from the (2 2 0) peaks of MgO and the (1 0 1) peaks of MgB_2 , respectively.

MgB_2 , and the volume expansion in Al-Ag codoped MgB_2 cannot induce T_c enhancement in the doped system, as shown in Fig. 3(b). Deemyad *et al.* have estimated the T_c dependence on unit cell volume for MgB_2 samples under pressure as $T_c(V) = \frac{dT_c}{d \ln V} = -\frac{B}{T_c(0)} \left(\frac{dT_c}{dP} \right) = +4.18$ using the bulk modulus $B = 147.2$ GPa, $T_c(0) = 39.1$ K, and $dT_c/dP \cong -1.11$ K/GPa.¹¹ As for the chemical doping effects, the SiC- and C-doped MgB_2 shows higher $T_c(V)$ values, from +4.5 at low doping levels to +12 at high doping levels, due to the extra electrons. Although the Al-Ag codoped MgB_2 keeps the system in electron balance, its $T_c(V)$ value is ~ -17.65 , which shows a different trend from the unit cell volume contraction systems.

For element doped MgB_2 , the phonon frequency decreases with the lattice cell volume expansion, which is consistent with the lattice cell volume variation due to external pressure. This can be described by the Grüneisen relation

$$\frac{d\omega_{E_{2g}}}{\omega_{E_{2g}}} = -\gamma \frac{dV}{V}, \quad (1)$$

where $\omega_{E_{2g}}$ is the vibration frequency, V is the relevant unit cell volume, $d\omega_{E_{2g}}$ and dV are the variations in $\omega_{E_{2g}}$ and V due to the substitutions, and γ is the Grüneisen parameter. Figure 4 plots the relationship between the frequency of the E_{2g} mode and the unit cell volume for the SiC-, carbon-, and Al-Ag-doped MgB_2 . The undoped samples processed under different conditions show different unit cell volumes and phonon frequencies. The unit cell volume of pure MgB_2 in Ref. 1, 29.06 Å³, is also shown in Fig. 4 for comparison. The SiC-doped samples show high Grüneisen parameters because both carbon substitution and inclusions can cause great crystal distortion.⁴⁶ The C-doped samples show slowly increased phonon frequency with decreased unit cell volume. An approximately linear variation with the Grüneisen parameter, $\gamma = 2.0$ – 4.0 , can be deduced for the doped MgB_2 , which is consistent with the values for pure MgB_2 under high pressure that were measured by Goncharov *et al.*,²⁵ $\gamma = (K_0 d \ln \omega / dP) = 2.9 \pm 0.3$, but larger than the results of Martinho *et al.*³²

For the strong electron-phonon coupling superconductors, the T_c can be predicted by the McMillan equation,⁴⁷ as modified by Allen and Dynes.⁴⁸

$$T_c = \frac{\langle \omega \rangle}{1.2} \exp \left(\frac{-1.04(1 + \lambda)}{\lambda - \mu^*(1 + 0.62\lambda)} \right), \quad (2)$$

where $\langle \omega \rangle$ is the averaged phonon frequency, λ is the electron-phonon coupling constant, and μ^* is the Coulomb pseudopotential. The electron-phonon coupling constant can be written as $\lambda = N(E_f) \langle I^2 \rangle (M \langle \omega^2 \rangle)^{-1}$, where $N(E_f)$ is the density of electron states at the Fermi energy E_f , $\langle I^2 \rangle$ is the square of the electron-phonon matrix averaged over the Fermi surface, M is the mass of the atom, and $\langle \omega^2 \rangle$ is the average value of the square of a characteristic phonon frequency. Deemyad *et al.* have deduced $T_c(V)$ on the basis of Eqs. (1) and (2),¹¹

$$\frac{d \ln T_c}{d \ln V} = -\gamma - \Delta_1 \left(\frac{\partial \ln \mu^*}{\partial \ln V} \right) + \Delta_2 \left(\frac{\partial \ln \eta}{\partial \ln V} + 2\gamma \right), \quad (3)$$

where $\eta = N(E_f) \langle I^2 \rangle$ is the McMillan-Hopfield parameter given by the product of the electronic density of states and

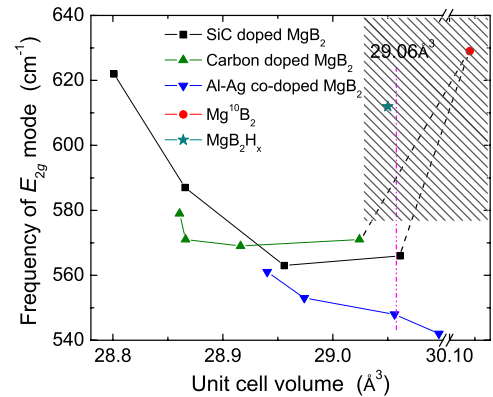


FIG. 4. (Color online) Dependence of the frequency of the E_{2g} mode on the unit cell volume for SiC-, carbon black, and Al-Ag-doped MgB_2 , for Mg^{10}B_2 , and for hydrogenated MgB_2 . The SiC-doped samples were sintered at 750 °C for 30 min. The carbon-doped samples were sintered at 900 °C for 2 h.^{8,15} The Al-Ag-doped MgB_2 was sintered at 950 °C for 1 h.³ The Mg^{10}B_2 sample was sintered at 950 °C for 2 h.^{40,51} The dashed black lines are guides for the Grüneisen relationship between the normal MgB_2 and Mg^{10}B_2 , and the magenta line (dash-dotted-dash-dotted) shows the unit cell volume value of pure MgB_2 in Ref. 1. The hydrogenated MgB_2 was processed in 30 atm H_2 atmosphere at 500 °C for 2 h. The shaded area is the predicted higher T_c position.

the average squared electronic matrix element, while the dimensionless prefactors $\Delta_1 = 1.04\mu^*(1+\lambda)(1+0.62\lambda)/[\lambda - \mu^*(1+0.62\lambda)]^2$ and $\Delta_2 = 1.04\lambda(1+0.38\mu^*)/[\lambda - \mu^*(1+0.62\lambda)]^2$ are calculated using the values of λ and μ^* at ambient pressure. The differences in the $d \ln T_c / d \ln V$ values between the V increasing and V decreasing systems [as calculated from Fig. 3(a)] is dominated by η for small changes of μ^* and γ in the doped MgB_2 (as shown in Fig. 4), which is similar to the explanation for the absence of superconductivity in LiB (Ref. 49) and Li_xBC ,⁵⁰ which is attributed to a reduction in the electronic density of states that is driven by the lattice structure vibration. This means that the chemical doping effects will decrease the electronic density of states for alien atom invasion, and this is the reason why the superconductivity cannot be increased solely by enhancing the phonon frequency and lattice parameters.

Of itself, the chemical doping tends to increase anharmonicity in the lattice, but the changes in the electronic density of states compensate for this, so that the harmonicity-anharmonicity balance is maintained. Although the chemical doping effect on superconductivity is disappointing, there are possible methods to break through this harmonicity-anharmonicity obstacle, which are hinted at by the isotope effect.⁵¹ Mg^{10}B_2 shows a higher T_c of 40.2 K than that of Mg^{11}B_2 at 39.2 K, while its cell volume, 30.11 \AA^3 ($a=3.1432 \text{ \AA}$, $c=3.5193 \text{ \AA}$, $c/a=1.1197$), as shown in Figs. 3(a) and 4, is larger than that of Mg^{11}B_2 ($a=3.086 \text{ \AA}$, $c=3.524 \text{ \AA}$, $c/a=1.142$, $V=29.06 \text{ \AA}^3$). It must be noted that the E_{2g} frequency of Mg^{10}B_2 is 629 cm^{-1} under ambient pressure, as shown in Figs. 3(b) and 4.⁴⁰ It is clear from comparison with the results plotted in Fig. 4 that higher T_c performance is achieved in expanded crystal cells with a higher E_{2g} frequency. Thus, the superconductivity can be enhanced in a negative Grüneisen parameter system if we set the phonon frequency and unit cell volume of pure MgB_2 as the starting point, as guided by the black dashed line in Fig. 4. The proper elements to enhance both the cell volume and E_{2g} frequency are expected to lead to a promising high T_c for MgB_2 . According to Eq. (3), the high electronic density of states and negative Grüneisen parameter are responsible for the high T_c in Mg^{10}B_2 .

To confirm the T_c dependence on the frequency of the E_{2g} mode and the unit cell volume, a pure MgB_2 sample was sintered at 800°C for 10 h to eliminate the second sintering effects on its T_c . Then the sample was processed at 500°C for 2 h in 30 atm H_2 atmosphere for hydrogenation. The unit cell volume calculated from the XRD pattern showed a small increase from 29.00 \AA^3 ($a=3.0839 \text{ \AA}$, $c=3.5208 \text{ \AA}$) to 29.05 \AA^3 ($a=3.0857 \text{ \AA}$, $c=3.5232 \text{ \AA}$), due to the hydrogen atoms, which are incorporated into the MgB_2 matrix and form MgB_2H_x as interstitial atoms, but not substitutional atoms. Nakamori *et al.* have compared the unit cell volume of sintered MgB_2 in argon and hydrogen. The lattice parameter a was nearly 0.1% larger in the sample sintered under hydrogen than in the sample sintered under argon. The T_c for the hydrogenated sample was $\sim 0.6 \text{ K}$ higher.⁵² The results of this work are in agreement with theirs. The phonon frequency of the E_{2g} mode measured from the Raman spectra increases, as shown in Fig. 5. The E_{2g} mode is dominant in the normal MgB_2 , because the long sintering makes the ma-

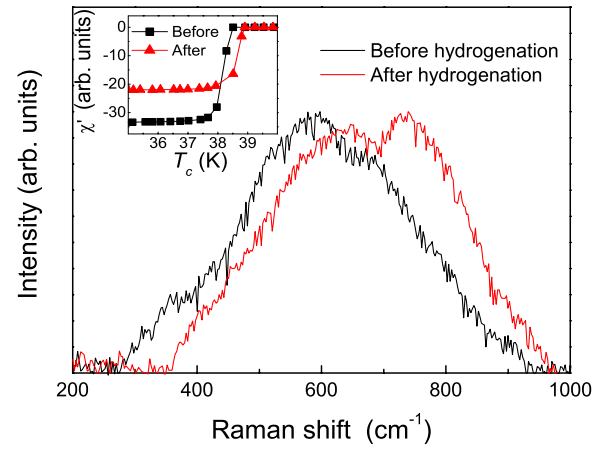


FIG. 5. (Color online) Normalized Raman spectra for MgB_2 before and after hydrogenation in 30 atm H_2 atmosphere at 500°C for 2 h. The baselines have been subtracted from the patterns. The inset shows the ac susceptibility of pure MgB_2 before and after hydrogenation, respectively.

terial harmonic, while the PDOS peak becomes obvious for the hydrogenated sample, since the interstitial H atoms cause anharmonicity in the crystal. The Gaussian fitted results for the E_{2g} mode and PDOS show that their frequencies shift from 587 and 754 cm^{-1} to 612 and 773 cm^{-1} , respectively. Both the phonon frequency and the unit cell volume have increased for the MgB_2 sample after hydrogenation. The trend breaks through the Grüneisen relationship which is obeyed by doped MgB_2 under high pressure. The peak shift is attributed to the decreased amplitude of the B atoms due to the confined vibration space arising from the interstitial H atoms in the lattice. Although Hirsch predicted a higher T_c exists with a shorter B-B intraplane distance under the application of in-plane biaxial pressure based on the hole model of superconductivity,⁵³ this prediction has not yet been confirmed experimentally because no uniaxial pressure measurement has been reported. The interstitial H atoms may introduce this kind of pressure into the MgB_2 lattice, shortening the actual distance of action between B atoms within a B plane, despite the expanded lattice parameter. In agreement with the above analysis, the hydrogenated sample shows a higher T_c of 38.9 K , an increase of $\sim 0.4 \text{ K}$, as shown in the inset of Fig. 5. The relationship between the phonon frequency and the unit cell volume is located in the shaded region in Fig. 4.

The most notable feature of the E_{2g} mode in the hydrogenated MgB_2 is the increase in both the frequency and the linewidth. The fitted FWHM value of the E_{2g} mode for the hydrogenated sample in Fig. 5 is 215 cm^{-1} , which is higher than that of the original sample, 204 cm^{-1} . Since the phonon linewidth is usually believed to be a signal of the intensity of the electron-phonon coupling, especially since the E_{2g} mode is considered the most relevant phonon in the superconducting transition, the increase in FWHM could be related to the T_c improvement. The intensity of electron-phonon coupling and crystal distortion will influence the Raman shift and the linewidth of the Raman scattering, which can give some insight into the harmonicity-anharmonicity competition be-

tween the E_{2g} mode and the other modes. Although the crystal distortion is obviously reflected by the strong PDOS peak in the Raman spectrum of the hydrogenated MgB_2 , the high frequency and strong FWHM of the E_{2g} mode indicates that the interstitial H atoms can strengthen the electron-phonon coupling at the same time. On the fact that the superconductivity is absent in most compounds with typical graphitelike structures, such as AlB_2 , ZrB_2 , NbB_2 , MoB_2 , YB_2 , TaB_2 , TiB_2 , HfB_2 , VB_2 , and CrB_2 , Calandra *et al.* believe that even small variations in the valence or mass of the intercalant or in the structural parameters of the boron layers are sufficient to considerably alter the σ or π and positions or the shape of their Fermi surfaces and consequently destroy superconductivity.⁴⁹ In contrast with the other chemical doping effects, H atoms do not substitute into the lattice positions of either Mg or B, where the dopant atoms lead to the formation of secondary phase particles and cause significant anharmonicity and distortion in the crystal lattice, which in turn reduce the T_c .⁵⁴ MgB_2H_x keeps the shape of the Fermi surface and the $N(E_F)$ with the absence of band filling. Furthermore, it shows strong electron-phonon coupling related to the increased frequency and linewidth of the E_{2g} mode. On the basis of hydrogenation experiments and the isotope effect, it is believed that the MgB_2 will have higher T_c if the values of the phonon frequency and the unit cell volume coincide with the shaded area in Fig. 4.

In summary, the doping effects of SiC, C, Mn, and Al-Ag on the T_c of MgB_2 strongly depend on the harmonicity-anharmonicity competition in the compounds. The phonon frequency changes to counteract the crystal lattice variation

to keep the system stable within a Grüneisen parameter of $\gamma=2.0-4.0$. Namely, the phonon frequency decreases as the unit cell volume is expanded, and *vice versa*. It is concluded from the $T_c(V)$ analysis that the decreased electronic density of states is responsible for the T_c depression in the doped MgB_2 . The T_c for pure MgB_2 can be improved by 0.4 K by hydrogenation in 30 atm H_2 atmosphere at 500 °C for 2 h. The interstitial H atoms in the MgB_2 lattice do not alter the shape of the Fermi surface and the density of electron states at the Fermi energy $N(E_F)$ due to the absence of element substitution for Mg or B. However, they enhance the E_{2g} mode and the intraplane B interaction. The strong increase in frequency and linewidth of the E_{2g} mode and the expanded unit cell volume of MgB_2H_x are responsible for the T_c increase in the material, which is different from the case of the other doped systems, where strong electron-phonon coupling and a large unit cell volume cannot coexist. Although extensive research has not found an effective way to enhance the T_c dramatically in the Mg-B system, there is reason to believe that it is possible to break through the harmonicity-anharmonicity obstacle and thus achieve high T_c MgB_2 compounds with both high phonon frequency and an expanded unit cell volume.

The authors appreciate useful discussions with T. Silver, Z.P. Guo, and J. Chen. The authors also acknowledge the Natural Science Foundation of China (Grant No. 50471100), the Australian Research Council, Hyper Tech Research, Inc., and CMS Alphatech International, Ltd. for their financial support.

*Author to whom correspondence should be addressed; shi@uow.edu.au

¹J. Nagamatsu, N. Nakagawa, T. Muranaka, Y. Zenitani, and J. Akimitsu, *Nature (London)* **410**, 63 (2001).

²M. L. Cohen, *J. Supercond. Novel Magn.* **19**, 283 (2006).

³L. Shi, H. R. Zhang, S. M. Zhou, J. Y. Zhao, and J. Zuo, *J. Appl. Phys.* **100**, 023905 (2006).

⁴R. H. T. Wilke, S. L. Bud'ko, P. C. Canfield, J. Farmer, and S. T. Hannahs, *Phys. Rev. B* **73**, 134512 (2006).

⁵C. S. Lue, T. H. Su, B. X. Xie, S. K. Chen, J. L. MacManus-Driscoll, Y. K. Kuo, and H. D. Yang, *Phys. Rev. B* **73**, 214505 (2006).

⁶D. Di Castro, M. Ortolani, E. Cappelluti, U. Schade, N. D. Zhigadlo, and J. Karpinski, *Phys. Rev. B* **73**, 174509 (2006).

⁷S. M. Kazakov, M. Angst, and J. Karpinski, *Solid State Commun.* **119**, 1 (2001).

⁸T. Takenobu, T. Ito, D. H. Chi, K. Prassides, and Y. Iwasa, *Phys. Rev. B* **64**, 134513 (2001).

⁹S. Lee, T. Masui, A. Yamamoto, H. Uchiyama, and S. Tajima, *Physica C* **397**, 7 (2003).

¹⁰J. Kortus, O. V. Dolgov, R. K. Kremer, and A. A. Golubov, *Phys. Rev. Lett.* **94**, 027002 (2005).

¹¹S. Deemyad, T. Tomita, J. J. Hamlin, B. R. Beckett, J. S. Schilling, D. G. Hinks, J. D. Jorgensen, S. Lee, and S. Tajima, *Physica C* **385**, 105 (2003).

¹²X. J. Chen, H. Zhang, and H. U. Habermeier, *Phys. Rev. B* **65**, 144514 (2002).

¹³J. M. An and W. E. Pickett, *Phys. Rev. Lett.* **86**, 4366 (2001).

¹⁴B. Gahtori, R. Lal, S. K. Agarwal, Y. K. Kuo, K. M. Sivakumar, J. K. Hsu, J. Y. Lin, A. Rao, S. K. Chen, and J. L. MacManus-Driscoll, *Phys. Rev. B* **75**, 184513 (2007).

¹⁵J. Arvanitidis, K. Papagelis, K. Prassides, G. A. Kourouklis, S. Ves, T. Takenobu, and Y. Iwasa, *J. Phys. Chem. Solids* **65**, 73 (2004).

¹⁶A. H. Moudden, *J. Phys. Chem. Solids* **67**, 115 (2006).

¹⁷T. Masui, S. Lee, and S. Tajima, *Phys. Rev. B* **70**, 024504 (2004).

¹⁸A. Bharathi, Y. Hariharan, J. Balaseli, and C. S. Sundar, *Sadhana-Acad. Proc. Eng. Sci.* **28**, 263 (2003).

¹⁹Y. Yan and M. M. Al-Jassim, *J. Appl. Phys.* **92**, 7687 (2002).

²⁰A. Q. R. Baron, H. Uchiyama, S. Tsutsui, Y. Tanaka, D. Ishikawa, J. P. Sutter, S. Lee, S. Tajima, R. Heid, and K. P. Bohnen, *Physica C* **456**, 83 (2007).

²¹S. X. Dou, S. Soltanian, J. Horvat, X. L. Wang, S. H. Zhou, M. Ionescu, H. K. Liu, P. Munroe, and M. Tomsic, *Appl. Phys. Lett.* **81**, 3419 (2002).

²²N. Suemitsu, T. Masui, S. Lee, and S. Tajima, *Physica C* **445-448**, 39 (2006).

²³K. P. Bohnen, R. Heid, and B. Renker, *Phys. Rev. Lett.* **86**, 5771 (2001).

- ²⁴J. Hlinka, I. Gregora, J. Pokorný, A. Plecenik, P. Kus, L. Satrapinsky, and S. Benacka, *Phys. Rev. B* **64**, 140503(R) (2001).
- ²⁵A. F. Goncharov, V. V. Struzhkin, E. Gregoryanz, J. Hu, R. J. Hemley, H. K. Mao, G. Lapertot, S. L. Bud'ko, and P. C. Canfield, *Phys. Rev. B* **64**, 100509(R) (2001).
- ²⁶K. P. Meletov, M. P. Kulakov, N. N. Kolesnikov, J. Arvanitidis, and G. A. Kourouklis, *JETP Lett.* **75**, 406 (2002).
- ²⁷P. Postorino, A. Congeduti, P. Dore, A. Nucara, A. Bianconi, D. Di Castro, S. De Negri, and A. Saccone, *Phys. Rev. B* **65**, 020507(R) (2001).
- ²⁸T. Yildirim, O. Gulseren, J. W. Lynn, C. M. Brown, T. J. Udovic, Q. Huang, N. Rogado, K. A. Regan, M. A. Hayward, J. S. Slusky, T. He, M. K. Haas, P. Khalifah, K. Inumaru, and R. J. Cava, *Phys. Rev. Lett.* **87**, 037001 (2001).
- ²⁹R. Osborn, E. A. Goremychkin, A. I. Kolesnikov, and D. G. Hinks, *Phys. Rev. Lett.* **87**, 017005 (2001).
- ³⁰D. Di Castro, E. Cappelluti, M. Lavagnini, A. Sacchetti, A. Palenzona, M. Putti, and P. Postorino, *Phys. Rev. B* **74**, 100505(R) (2006).
- ³¹L. Shi, H. R. Zhang, L. Chen, and Y. Feng, *J. Phys.: Condens. Matter* **16**, 6541 (2004).
- ³²H. Martinho, C. Rettori, P. G. Pagliuso, A. A. Martin, N. O. Moreno, and J. L. Sarrao, *Solid State Commun.* **125**, 499 (2003).
- ³³M. Calandra, M. Lazzeri, and F. Mauri, *Physica C* **456**, 38 (2007).
- ³⁴A. Shukla, M. Calandra, M. d'Astuto, M. Lazzeri, F. Mauri, C. Bellin, M. Krisch, J. Karpinski, S. M. Kazakov, J. Jun, D. Daghero, and K. Parlinski, *Phys. Rev. Lett.* **90**, 095506 (2003).
- ³⁵M. d'Astuto, M. Calandra, S. Reich, A. Shukla, M. Lazzeri, F. Mauri, J. Karpinski, N. D. Zhigadlo, A. Bossak, and M. Krisch, *Phys. Rev. B* **75**, 174508 (2007).
- ³⁶A. Q. R. Baron, H. Uchiyama, Y. Tanaka, S. Tsutsui, D. Ishikawa, S. Lee, R. Heid, K. P. Bohnen, S. Tajima, and T. Ishikawa, *Phys. Rev. Lett.* **92**, 197004 (2004).
- ³⁷M. Eisterer, R. Müller, K. Schöpl, H. W. Weber, S. Soltanian, and S. X. Dou, *Supercond. Sci. Technol.* **20**, S117 (2007).
- ³⁸S. X. Dou, O. Shcherbakova, W. K. Yeoh, J. H. Kim, S. Soltanian, X. L. Wang, C. Senatore, R. Flukiger, M. Dhalke, O. Husnjak, and E. Babic, *Phys. Rev. Lett.* **98**, 097002 (2007).
- ³⁹K. Prassides, Y. Iwasa, T. Ito, D. H. Chi, K. Uehara, E. Nishibori, M. Takata, S. Sakata, Y. Ohishi, O. Shimomura, T. Muranaka, and J. Akimitsu, *Phys. Rev. B* **64**, 012509 (2001).
- ⁴⁰A. F. Goncharov and V. V. Struzhkin, *Physica C* **385**, 117 (2003).
- ⁴¹T. Tomita, J. J. Hamlin, J. S. Schilling, D. G. Hinks, and J. D. Jorgensen, *Phys. Rev. B* **64**, 092505 (2001).
- ⁴²B. Lorenz, R. L. Meng, and C. W. Chu, *Phys. Rev. B* **64**, 012507 (2001).
- ⁴³E. Saito, T. Takkenoby, T. Ito, Y. Iwasa, K. Prassides, and T. Arima, *J. Phys.: Condens. Matter* **13**, L267 (2001).
- ⁴⁴R. Falconi, A. Durán, and R. Escudero, *J. Phys.: Condens. Matter* **14**, 3663 (2002).
- ⁴⁵J. Tang, L. C. Qin, H. W. Gu, A. Matsushita, Y. Takano, K. Togano, H. Kito, and H. Ihara, *J. Phys.: Condens. Matter* **14**, 10623 (2002).
- ⁴⁶X. L. Wang, S. Soltanian, M. James, M. J. Qin, J. Horvat, Q. W. Yao, H. K. Liu, and S. X. Dou, *Physica C* **408**, 63 (2004).
- ⁴⁷W. L. McMillan, *Phys. Rev.* **167**, 331 (1968).
- ⁴⁸P. B. Allen and R. C. Dynes, *Phys. Rev. B* **12**, 905 (1975).
- ⁴⁹M. Calandra, A. N. Kolmogorov, and S. Curtarolo, *Phys. Rev. B* **75**, 144506 (2007).
- ⁵⁰A. M. Fogg, J. Meldrum, G. R. Darling, J. B. Claridge, and M. J. Rosseinsky, *J. Am. Chem. Soc.* **128**, 10043 (2006).
- ⁵¹S. L. Bud'ko, G. Lapertot, C. Petrovic, C. E. Cunningham, N. Anderson, and P. C. Canfield, *Phys. Rev. Lett.* **86**, 1877 (2001).
- ⁵²Y. Nakamori, S. Orimo, T. Ekino, and H. Fujii, *J. Alloys Compd.* **335**, L21 (2002).
- ⁵³J. E. Hirsch, *Phys. Lett. A* **282**, 392 (2001).
- ⁵⁴D. W. Gu, Y. M. Cai, J. K. F. Yau, Y. G. Cui, T. Wu, G. Q. Yuan, L. J. Shen, and X. Jin, *Physica C* **386**, 643 (2003).